

Chapter 6

EXPERIMENTAL RESULTS

This chapter reports the horizontal pressure increment against a 1.5 m-high non-yielding wall induced by flexible and rigid surcharge loadings. Loose Ottawa sand with unit weight γ of 15.6 kN/m^3 is used as backfill for the experiments. Based on direct shear tests, the internal friction angle ϕ for the loose backfill is 31.2° . The γ and ϕ values are used to calculate the Jaky's earth pressure coefficient. The horizontal distances from center of the strip footing to the face of the model wall adopted in the experiments are 0.15 m, 0.30 m, and 0.60 m. For a wall height $H = 1.5\text{m}$, the corresponding parameter m is 0.1, 0.2, and 0.4 respectively. Surcharge loading is applied on the top of backfill, and the induced earth-pressure is monitor with soil pressure transducers on the NCTU non-yielding model wall facility. Testing Programs are listed on Table 6.1.

6.1 Earth Pressure At-Rest

In this section, experimental results of the earth pressure at-rest were measured by soil pressure transducer (SPT) after the backfill was filled up to 1.5 m. The relative density achieved for the loose backfill was 35% respectively. The method of air-pluviation was adopted for all tests to prepare the backfill. As shown in Fig. 6.1, the experimental earth pressure at-rest for Test0518, 0526, 0609, and 0610 are compared with Jaky's solution for loose sand. In this figure, the earth pressure distribution tends

to be linear and in fairly good agreement with Jaky's equation. Mayne and Kulhawy (1982), Mesri and Hayat (1993) reported that Jaky's equation is suitable for backfill in its loosest state. The point of application of the at-rest thrust would act at about on third of the wall height $H/3$ above the base.

6.2 Ultimate Bearing Capacity of Loose Sand

In order to apply an appropriate surcharge intensity q on the top of the backfill, it is necessary to determine the ultimate bearing capacity q_{ult} of the air-pluviated loose sand. As shown in Fig. 6.2, the surcharge loading system was used to establish the loading - settlement relationship for the strip footing. The bearing capacity test was conducted on the surface of the 1.5 m x 1.5 m x 1.5 m backfill and the centerline of footing was placed at 0.75 m from the face of the wall.

In Fig. 6.3, Vesic (1973) defined three types of the bearing failure mode with the soil density and the depth of embedment of footing. Typical failure modes of a footing includes: punch shear failure, local shear failure, and general shear failure. The load – settlement relationships for these failure modes are shown in Fig.6.4. The relative density of backfill in this study is about 35% and the loading was applied on the surface of the backfill ($D_f = 0$). Based on Fig. 6.3, it is clear that the punching shear failure would occur.

The experimental load-settlement relationships due to the application of flexible and rigid strip loads are shown in Fig. 6.5. Like the $q - S$ relationship shown in Fig. 6.4(c), the settlement increases with increasing loading. There is no obviously peak loading measured during the loading process. As there was no reliable theory for

estimating the ultimate bearing capacity of punching failure, the experimental results reported by Vesic (1963) and Das (1994) are taken into consideration. Das (1994) reported that the ultimate bearing capacity q_{ult} of footing can be defined as the loading corresponding to $S = 0.15B \sim 0.25B$, where S is settlement of the strip footing and B is the width of strip footing. Following this definition, based on Fig. 6.5, the ultimate bearing capacity for the strip footing on loose sand $q_{ult} = 24.1 \sim 30.1 \text{ kN/m}^2$ is suggested for the flexible footing.

The load – settlement relationship due to the application of a rigid strip loading is also shown in Fig. 6.5. The test data are quite close to that obtained for the flexible footing. The strip loading corresponding to $S = 0.15B$ and $0.25B$ are 24.4 and 31.3 kN/m^2 , respectively. From a conservative point of view, $q_{ult} = 24.1 \text{ kN/m}^2$ is selected for a strip footing on loose sand. If a factor of safety $FS = 3.0$ is used, the allowable bearing capacity $q_{all} = 8.03 \text{ kN/m}^2$ could be obtained. For experiments in the following sections, $q_{all} = 0.333q_{ult} = 8.03 \text{ kN/m}^2$ will be the limit value of vertical surcharge loading to apply on the surface of backfill.

6.3 Lateral Pressure Due to Flexible Footing

The lateral earth pressure $\Delta\sigma_h$ on the non-yielding wall induced by a flexible surcharge loading is investigated in the section. The measured distribution of horizontal pressure increase is compared with $\Delta\sigma_h$ estimated with the DM 7.2 manual and the method of image.

Besides the distribution of lateral pressure increment, the magnitude of horizontal resultant force increment ΔP_h and the point of application of ΔP_h would be interest to engineers. In Fig. 6.6 R is the vertical distance measured from the base of wall to the

load increment ΔP_h . The strip loading is located at mH from the face of the wall. In Fig. 6.6, H is the height of wall and B is the width of footing. The parameter m used in this study includes 0.1, 0.2 and 0.4. The surcharge loading applied includes $0.11q_{ult}$, $0.22q_{ult}$ and $0.33q_{ult}$. The coefficient of horizontal thrust increment due to the strip surcharge q is defined as follows:

$$\Delta K_h = \frac{\Delta P_h}{qB} \quad (6.1)$$

where B is the width of strip footing. The horizontal thrust increment ΔP_h is calculated by summing the pressure diagram shown in Fig. 6.6.

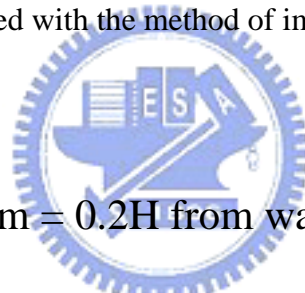
6.3.1 Strip Loading at $m = 0.1H$ from wall

Fig. 6.7(a) shows the distribution of horizontal pressure increase $\Delta\sigma_h$ due to the application of a flexible strip surcharge $q = 0.11q_{ult}$ located at 0.15 m from the face of wall ($m = 0.1$). It is clear in the figure that the $\Delta\sigma_h$ measure near the top of the wall is significantly greater than that estimated with the method of image and design manual DM 7.2. For this case, the surcharge loading is quite close ($m = 0.1$) to the face of the wall. However, Terzaghi (1954) suggested that for value of m less than 0.4, pressure on the wall due to the line load q should be determined as $m = 0.4$. The distribution of $\Delta\sigma_h$ shown in Fig. 6.7(a) is actually that for $m = 0.4$. From a practical point of view, it would be reasonable to expect $\Delta\sigma_h$ measured at SPT15 (Fig. 3.3) would increase with the approaching of surcharge loading q . The relationship of σ_h and $\Delta\sigma_h$ is shown in Fig. 6.7(d).

The distribution of horizontal pressure increase $\Delta\sigma_h$ due to the application of surcharge $q = 0.22q_{ult}$ and $0.33q_{ult}$ is shown in Fig 6.7(b) and Fig 6.7(c), respectively, It is found that the measured $\Delta\sigma_h$ distribution is in fairly good agreement with those

calculated with the method of image. However, the DM 7.2 method significantly underestimated the horizontal pressure increase near the top of the wall. Based on the test data, it may be concluded that, for $m = 0.1$, the $\Delta\sigma_h$ due to strip surcharge can be properly estimated with the method of image. However, the DM 7.2 method based on $m = 0.4$ failed predict the horizontal pressure increase due to a strip surcharge loading.

The variation horizontal soil thrust coefficient ΔK_h at three different loading stages are in fairly good agreement with the predication based on method of image for $q = 0.22q_{ult}$ and $0.33q_{ult}$. However, the extra high stress measured at SPT15 cause an extremely high ΔK_h value for $q = 0.11q_{ult}$. The location of the point of application of the resultant force ΔP_h is illustrated in Fig. 6.9. The test results are in very good agreement with those calculated with the method of image.



6.3.2 Strip Loading at $m = 0.2H$ from wall

Fig. 6.10(a) shows the distribution of $\Delta\sigma_h$ due to the flexible surcharge $q = 0.11q_{ult}$ located at 0.30 m from the face of wall ($m = 0.2$). The measured horizontal pressure increment $\Delta\sigma_h$ near the top of backfill slightly greater than that calculated with the method of image. The surcharge loading is still quite close ($m = 0.2$) to the face of the wall. The DM 7.2 method based on the $m = 0.4$ still fails to predict the horizontal pressure increase due to a strip loading for $m = 0.2$.

The distribution of horizontal pressure increase $\Delta\sigma_h$ due to the application of surcharge $q = 0.22q_{ult}$ is shown in Fig. 6.10(b). It is clear that the $\Delta\sigma_h$ measured near the top of the wall is slightly less than that estimated with method of image, but greater than that estimated with the DM 7.2 manual. In Fig 6.10(c), the distribution of $\Delta\sigma_h$ due to surcharge loading $q = 0.33q_{ult}$ is shown. Based on test data, the measured $\Delta\sigma_h$ near the top of the backfill is lower than that estimated with the method of image. It is clear

in the figure that the measured $\Delta\sigma_h$ near the depth of 0.5 m is lower than the theoretical solutions. It should be noted in Fig. 6.10(a) (b) and (c) that the peak $\Delta\sigma_h$ measured at SPT14 is 0.478, 0.657, and 0.836 kN/m², respectively. These values do not increase linearly with the linear increase of surcharge loading $q = 0.11, 0.22$ and $0.33q_{ult}$. In the elastic theory, the soil mass is assumed to be homogeneous, isotropic, linearly elastic, and does not change its properties in the shearing process.

The variation horizontal soil thrust coefficient ΔK_h with increasing surcharge loading q is shown in Fig. 6.11. The ΔK_h is 16% higher than the values of method of image at surcharge loading $q = 0.11q_{ult}$, 21% lower at $0.22q_{ult}$, and 33% lower at $0.33q_{ult}$. The point of application of the resultant force ΔP_h with increasing q is illustrated in Fig. 6.12. The test results are in good agreement with that calculated with the method of image.



6.3.3 Strip Loading at $m = 0.4H$ from wall

Since the surcharge is located at 0.6 m ($m = 0.4$) away from wall, the theoretical $\Delta\sigma_h$ values that suggested by DM 7.2 would be the same as that calculated with the method of image. The distribution of $\Delta\sigma_h$ due to the flexible surcharge $q = 0.11q_{ult}$ is shown in Fig. 6.13(a). For $z = 0.05$ m ~ 0.6 m, test result is exceeds that estimated with the method of image. In Fig. 6.13(b) and (c), the $\Delta\sigma_h$ measured near the top of the wall is relatively close to the theoretical solution. However, the measured $\Delta\sigma_h$ below the depth of 0.3 m is lower than the theoretical solution.

In Fig. 6.14, the measured horizontal thrust coefficient ΔK_h is 21% greater than the value estimated with the method of image at the surcharge loading $q = 0.11q_{ult}$. The measured ΔK_h is 17% and 35% lower than theoretical value at the surcharge loading of 0.22 and $0.33q_{ult}$, respectively. Fig. 6.15 shows the measured point of application of soil

thrust is located about 19% higher than the calculated location.

6.4 Lateral Pressure Due to Rigid Footing

6.4.1 Strip Loading at $m = 0.1H$ from wall

Fig. 6.16(a) shows the distribution of $\Delta\sigma_h$ due to a rigid strip loading $q = 0.22q_{ult}$ applied at the surface of backfill. The test data is in fairly good agreement with that calculated with the method of image. In the figure, the DM 7.2 equation apparently underestimated the $\Delta\sigma_h$ at upper 0.3 m of backfill, and it overestimated the $\Delta\sigma_h$ at lower 1.2m of backfill. The similar observation can also be obtained for the $\Delta\sigma_h$ distribution shown in Fig. 6.16(b). In the figure, the measured $\Delta\sigma_h$ does not increase appreciably with the increase of surcharge intensity from $0.22q_{ult}$ to $0.33q_{ult}$.

Fig. 6.17 shows the soil thrust coefficient ΔK_h due to the rigid surcharge at $m = 0.1$ can be properly predicted with the method of image. Fig. 6.18 shows the point of application of the horizontal force increment ΔP_h due to the rigid footing can be accurately estimated with the method of image.

6.4.2 Strip Loading at $m = 0.2H$ from wall

The distribution of horizontal pressure increase $\Delta\sigma_h$ due to the application of a rigid surcharge $q = 0.22q_{ult}$ located at 0.30 m from the face of the wall ($m = 0.2$) is shown in Fig. 6.19(a). It is found that the measured $\Delta\sigma_h$ is in fairly good agreement with that calculated with method of image, but greater than that calculated with the DM 7.2 at upper 0.4 m of backfill. Fig 6.19(b) shows the $\Delta\sigma_h$ due to the application of

surcharge $q = 0.33q_{ult}$. In the figure, the measured $\Delta\sigma_h$ at upper 0.5 m of backfill is slightly lower than that estimated with the method of image. However, the DM 7.2 method quite overestimated the $\Delta\sigma_h$ at lower 1.0 m of backfill.

In Fig. 6.20, the measured soil thrust coefficient ΔK_h is lower than the values estimated with the method of image. Fig 6.21 shows the point of application of the soil thrust ΔP_h is slightly higher than that estimated with either the method of image or DM7.2 equation.

6.4.3 Strip Loading at $m = 0.4H$ from wall

Fig. 6.22(a) shows the distribution of $\Delta\sigma_h$ due to the application of a rigid strip loading $q = 0.22q_{ult}$. At the depth less than 0.6 m, the experimental $\Delta\sigma_h$ values are in relatively good agreement with theoretical solution. At the depth greater than 0.6 m, the test results are obviously less than the theoretical solution. Similar observations can be obtained based on the test results shown in Fig. 6.22(b). Fig. 6.23 shows that the measured soil thrust coefficients ΔK_h are lower than the calculated with the method of image. Fig. 6.24 shows that the point of application of ΔP_h is located at a position slightly higher than expected. The phenomena obtained in Fig. 6.23 and 24 are most probably due to the low stresses measured at lower 0.9 m of backfill.

6.5 Effect of Surcharge Position

The variation of soil thrust coefficient ΔK_h as a function of position of surcharge m for $q = 0.11q_{ult}$, $q = 0.22q_{ult}$ and $q = 0.33q_{ult}$ is shown in Fig. 6.25, 26 and 27,

respectively. The ΔK_h values calculated with the method of image, DM 7.2 method, and elastic solution are also indicated in the figure. It is found that:

1. Both the experimental and theoretical ΔK_h increase with decreasing parameter m (the strip loading approaches the wall).
2. The test results due to the application of flexible and rigid footings are quite similar.

The variation of horizontal resultant for ΔP_h location as a function of surcharge location for $q = 0.11q_{ult}$, $q = 0.22q_{ult}$ and $q = 0.33q_{ult}$ is shown in Fig. 6.28, 29 and 30, respectively. Based on the test data, the following conclusion can be drawn.

1. Both the experimental and theoretical location of ΔP_h increase with decreasing parameter m . As the strip loading approaches the wall, the stress concentration zone under the footing moves closer to the unyielding wall, causing the $\Delta\sigma_h$ acting near the top of the wall to increase.
2. The Parameter R/H measured for $q = 0.11q_{ult}$, $q = 0.22q_{ult}$ and $q = 0.33q_{ult}$ are almost identical. Typical R/H values ranged between 0.73 and 0.85.
3. The experimental R/H values are equal to or greater than the R/H values calculated with the method of image. The DM 7.2 method would underestimate the point of application of the induced force increment ΔP_h .